ab initio calculated frequency-dependent nonlinear optical properties on CsGeBr3

L. C. Tang[a,b], Y.C. Chang[c,d], J. Y. Huang[b], and C. S. Chang[b]

[a]Department of Applied Physics, Chung-Cheng Institute of Technology, National Defense University, TaoYuan, 33509, Taiwan, ROC;
[b]Department of Photonics & Institute of Electro-Optical Engineering, National Chiao Tung University, Hsinchu 305, Taiwan, ROC;
[c]Department of Physics, University of Illinois at Urbana-Champaign, Urbana 61801 USA;
[d]Research Center for Applied Science, Academia Sinica, Taiwan, ROC

ABSTRACT

A systematic first-principles calculation of the linear and second-order optical susceptibilities as functions of frequency for $CsGeBr_3$ is presented. Specifically, we study the relation between the structural properties and the optical responses. Three structural deformation factors, $\Delta\alpha$, d_{Ge}, d_X are used to express the degree of distortion from the ideal perovskite structure in bond angle, Ge position, and anion position, respectively. Based on our first-Principles studies, we find that $\Delta\alpha$ and d_{Ge} increase, while d_X decreases as we substitute the halogen ion from Cl to Br and then to I. The dielectric function and the second harmonic generation coefficient are also found to increase with increasing $\Delta\alpha$ and d_{Ge}. Our calculation indicates that the direct bandgap, E_g, of $CsGeX_3$ occurs at the R-point for all three compounds, and its magnitude decreases as $\Delta\alpha$ and d_{Ge} increase (i.e. $E_g(CsGeI_3) < E_g(CsGeBr_3) < E_g(CsGeCl_3)$). Our partial density of states (PDOS) analysis reveals that the valence band maximun (VBM) and conduction band minimum (CBM) are mainly associated with the p-orbitals of Germanium. Interband and intraband analysed results for $\chi^{(2)}_{ijk}$ in $CsGeBr_3$ can be separated into two main groups of peaks. One was contributed from the magnitude electronic bandgap; the other part was recognized to be attribution from the distortional structural factors. The magnitudes of $\chi^{(2)}_{ijk}$ were in the same manner with some reported experiment near the band gap.

Keywords: First-Principles, chi2, frequency-dependent, second-order optical susceptibilities

1. INTRODUCTION

Second-order nonlinear optical (NLO) materials play a key role in many areas in optics, such as laser frequency conversion and optical parametric oscillation/amplification (OPO/OPA).[1,2] Recently, several ternary halides expressed as ABX_3 ($A = Cs, Rb$, $B = Ge, Cd$, $X = Cl, Br, I$)[3–10] were discovered to exhibit strong second-order NLO properties. Rhombohedral $CsGeCl_3$ (CGC), which was found to possess excellent second-order NLO properties, exhibits a second-harmonic generation (SHG) five times larger than that of KH_2PO_4 (KDP), and its damage threshold reaches $200MW/cm^2$.[8] The electronic structure and linear optical properties of $CsGeI_3$ (CGI) were reported by Tang *et al.*[6] Meanwhile, $CsCdBr_3$ was found by P. Ren *et al*[11] to be noncentrosymmetric, i.e. lack of inversion symmetry. Rhombohedral $CsGeBr_3$ (CGB), which was found to possess even better second-order NLO properties than CGC, exhibits a SHG about ten times larger than that of KDP.[10] The ternary halides, rhombohedral $CsGeX_3$ (CGX, X=Cl, Br, I), have recently become a new class of nonlinear optical (NLO) materials, which has potential device application from the visible to infrared. Furtehmore, there are some interesting aspects of the rhombohedral CGX crystals that are worth noting. First of all, the CGXs have similar crystal structure, and they all possess identical space group symmetry, i.e. R3m (160). Traditional

Further author information: (Send correspondence to Li-Chuan Tang)
L. C. Tang: E-mail: newton4538.eo85g@nctu.edu.tw, Telephone: +886 3 380 4538
C.S. Chang: E-mail: cschang@nctu.edu.tw, Telephone: +886 3 571 2121

Infrared and Photoelectronic Imagers and Detector Devices II, edited by Randolph E. Longshore, Ashok Sood,
Proc. of SPIE Vol. 6294, 62940J, (2006) · 0277-786X/06/$15 · doi: 10.1117/12.681410

Downloaded From: http://proceedings.spiedigitallibrary.org/ on 01/21/2013 Terms of Use: http://spiedl.org/terms

empirical equation such as the Goldschmidts tolerence factor[12,13] cannot properly predict their crystal structure. CGXs rhombohedrally deform from an ideal perovskite crystal structure. Second, they have large NLO susceptibility. Third, the transparent spectrum of CGX can be extended to much longer wavelength (20μm) in the infrared range. Therefore, CGX crystals have application in wider spectral range. The only drawback for CGX crystals is that large size and high quality crystals are difficult to grow.

In this paper, the frequency-dependent linear and nonlinear optical properties of $CsGeBr_3$ will be focused on. The second aspect mentioned above will be investigated. Systematic analysis on the effect of CGB crystal structure on their electronic and optical properties will be carried out. In order for this new class of NLO materials to be applicable for infrared SHG, it should possess the following attributes: transparency in the relevant wavelengths; ability to withstand laser irradiation, and chemical stability. Most importantly, the material of concern must be crystallographically noncentrosymmetric. Mathematically it has been known for some time that only a noncentrosymmetric arrangement of atoms may produce a second-order NLO response.[14–16]

Our calculations for the nonlinear response functions are based on the formalism given by Sipe and Ghahramani[17] and by Aversa and Sipe.[18] The independent particle approximation has been used. This approach has the advantage that the response coefficients are inherently free of any unphysical divergences at zero frequency. It does not need to invoke the 'Sum rules' to eliminate the artificial divergences. The recent work of Dal Corso and Mauri,[19] based on an elegant Wannier function approach, is also free of such divergences.

The full band structure calculation in this work utilized the norm-conserving pseudo-potential plane wave within the local density approximation (LDA). This method has an advantage over that employed by Moss and co-workers[20–24] in that it is first principles rather than semiempirical in nature. The local field effects in this work has not been included, since we do not expect such effects to lead to significant corrections for the materials considered here at the level of second-order response, as suggested by the work of Levine and Allan[25] . However, the inclusion of local field effects can be done in a straightforward way within our formalism for the response functions.

Table 1. Lattice constants and coordinates (in reduced units) of Ge and halogen atoms of Rhombohedral NLO crystals $CsGeX_3$.

	a	α	a_{Ge}	$X_{a,b,c}$	t_G
CGC (exp.)	5.434(2)	89.72(3)	0.481(0)	0.502400 0.502400 0.053800	1.027(2)
CGB (exp.)	5.635(9)	88.74(4)	0.476(4)	0.501800 0.501800 0.027100	1.009(4)
CGI (exp.)	5.983(0)	88.60(0)	0.470(3)	0.502900 0.502900 0.011900	0.984(6)
CGC (calc.)	5.510(8)	89.12(1)	0.479(9)	0.502848 0.502848 0.058529	
CGB (calc.)	5.688(5)	88.29(7)	0.470(9)	0.502245 0.502245 0.031737	
CGI (calc.)	5.998(4)	87.65(5)	0.464(6)	0.506888 0.506888 0.010163	

2. LATTICE DISTORTION AND OPTICAL RESPONSES

2.1. Structural Factors

The structural distortion was considered as one of the main contributing factors to the optical nonlinearity of $CsGeBr_3$. For perovskite-type (see Figure 1) ternary oxides ABO_3 as well as halides $CsGeX_3$, Goldschmidt's tolerance factor t_G[12,13] serves as a discriminating parameter for classifying perovskites in terms of structure modification and its resulting physical properties.[26–30] The tolerance factor t_G is defined as[12,13]

Downloaded From: http://proceedings.spiedigitallibrary.org/ on 01/21/2013 Terms of Use: http://spiedl.org/terms

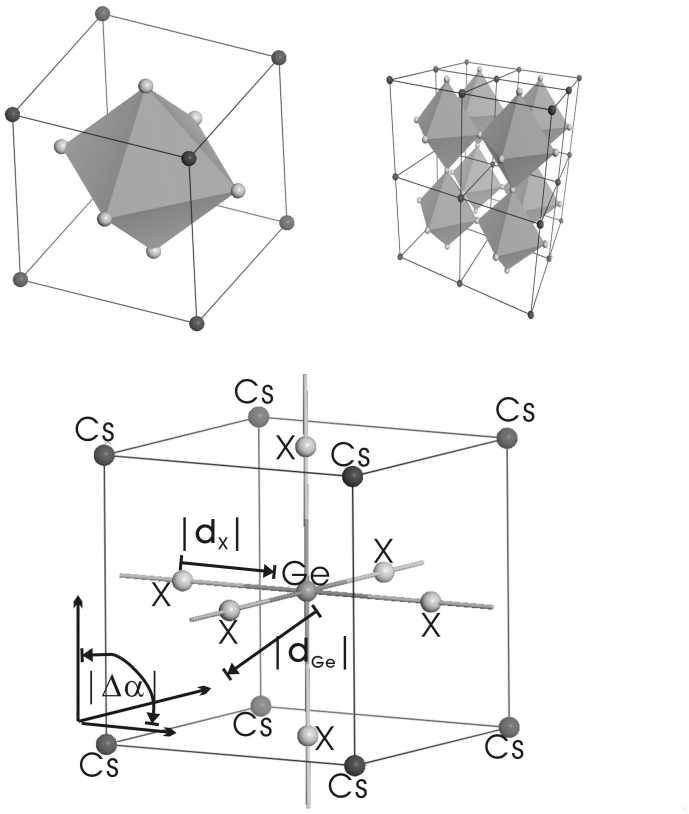

Figure 1. The crystal structure of rhombohedral $CsGeX_3$, which is distorted from an ideal perovskite structure. The upper-left illustration is a B-site cation center model. The upper-right is an A-site cation center model. The labels in the lower figure illustrate the proposed structural deformation factors.

$$t_G = \frac{(r_A + r_X)}{\sqrt{2} \cdot (r_B + r_X)}, \tag{1}$$

where A is a large cation, B a smaller one, X is the anion and the r are the ionic radii of Shannon and Prewitt,[31,32] which depend on the coordination number and bonding-specimens. An empirical rule was established[26–30] that a crystal structure should behave close to an ideal perovskite model when $0.97 \leq t_G \leq 1.03$. The structural parameters of $CsGeBr_3$, which were reported in,[33–37] are listed in Table 1. For comparison, the lattice constants and atomic positions of ternary halide crystals are also summarized in the lower half of Table 1. The tolerance factors, t_G of $CsGeX_3$ crystals are 1.009(4) 1.027, and 0.984, respectively. (see the far right column in Table 1). They are close to the empirically ideal perovskite structure with $t_G = 1.0$. According to the empirical rule, CGX crystals should behave like an ideal perovskite structure. However, $CsGeX_3$ crystals were all found to have the rhombohedral structure. This suggests that some extra structure factors need to be to considered in order to provide a better description.

First, it is noted that the lattice angles for CGX crystals reduce slightly and uniformly from the 90^0 lattice angle of an ideal perovskite structure. We define the angular distortion parameter

$$\Delta\alpha = \frac{(90 - \alpha_{rhomb})}{90} \times 100. \tag{2}$$

Downloaded From: http://proceedings.spiedigitallibrary.org/ on 01/21/2013 Terms of Use: http://spiedl.org/terms

Second, the smaller B-site cation, Germanium shifts away from the cell center along the diagonal axis toward the corner. We define the Ge displacement parameter as

$$d_{Ge}^{rhomb} = |(\vec{r}_{Ge}^{fc} - \vec{r}_{Ge}^{rhomb})| \times 100. \tag{3}$$

Finally, the displacement of halogen ions, X(=Cl, Br, and I) are described as

$$d_{X}^{rhomb} = |(\vec{r}_{X}^{fc} - \vec{r}_{X}^{rhomb})| \times 100, \tag{4}$$

where $\vec{r}$ denotes the position vector of ions in reduced coordinates. These structural deformation factors are also illustrated in Figure 1. The structural deformation factors obtained from experimental data and the first-principles calculations are listed in Table 2. As seen in Table. 2, $\Delta\alpha$ and d_{Ge} increase while d_X and t_G decrease with increasing atomic weight.

2.2. Optical response functions

For the linear susceptibility, we adopt the analytic expression given by[17]

$$\tilde{\chi}_I^{ab}(-\omega;\omega) = \frac{e^2}{\Omega\hbar}\sum_{nm\mathbf{k}} f_{nm}\frac{r_{nm}^a(\mathbf{k})r_{mn}^b(\mathbf{k})}{[\omega_{nm}(\mathbf{k}) + (\Delta/\hbar)(\delta_{mc} - \delta_{nc}) - \omega]}, \tag{5}$$

where n and m label energy bands; $f_{mn} \equiv f_m - f_n$, with f_i the Fermi occupation factor. $\mathbf{k}$ denote the wave vectors in the Brillouin zone. $\omega_{mn}(k) \equiv \omega_m(k) - \omega_n(k)$ denote the frequency differences. r_{mn} are the dipole matrix elements, which are related to the velocity matrix elements, v_{mn} via $r_{mn} = v_{mn}/(i\omega_{nm})$. Δ denotes the constant shift used in the 'scissors approximation' to correct the energy band gap difference caused by the local density approximation.

For the second-order response we write[17]

$$\chi^{abc}(-\omega_\beta - \omega_\gamma;\omega_\beta,\omega_\gamma) = \chi_{II}^{abc}(-\omega_\beta - \omega_\gamma;\omega_\beta,\omega_\gamma)$$
$$+\eta_{II}^{abc}(-\omega_\beta - \omega_\gamma;\omega_\beta,\omega_\gamma) + \frac{i}{(\omega_\beta + \omega_\gamma)}\sigma_{II}^{abc}(-\omega_\beta - \omega_\gamma;\omega_\beta,\omega_\gamma), \tag{6}$$

where χ_{II}^{abc} represents the purely interband contribution. η_{II}^{abc} describes the contribution from the modulation of the linear susceptibility by the intraband motion of the electrons. The third term is due to the modification of the intraband motion by the polarization energy associated with the interband transition. Explicit expressions for $\chi^{abc}(-2\omega : -\omega, -\omega)$ and $\chi^{abc}(-\omega : -\omega, 0)$ can be found in Appendix B of Ref.[17] To include the 'scissors operation' effect, we simply replace $\omega_{nm}(\mathbf{k})$ in these expressions by $\omega_{nm}(\mathbf{k}) + (\Delta/\hbar)(\delta_{mc} - \delta_{nc})$.

3. RESULTS AND DISCUSSION

Results for the calculated electronic band structure, projected density of state (PDOS), frequency-dependent dielectric function on xx and zz components of rhombohedral $CsGeBr_3$ were carried out and shown in figure 2. Partial densities of states (PDOS) of $CsGeBr_3$ projected onto all species at various atomic orbitals. There was found a direct-gap on R-point rather than Γ-point. *ab initio* calculated and the measured band gap values were also listed in Table 3. There were two significant peaks found in each linear optical susceptibily. First group of significant peaks were observed around the CGX bandgap values. The other group of peaks were deviated from and were higher than zero-photon-energy (frequency) according to the degree of distortion, e.g. $\epsilon_{Ge,cal}^{CGC} : \epsilon_{Ge,cal}^{CGB} : \epsilon_{Ge,cal}^{CGI} \approx 9 : 10 : 12$. Two further comments concerning $\epsilon"(\omega)$ were made: First, the intensity

Downloaded From: http://proceedings.spiedigitallibrary.org/ on 01/21/2013 Terms of Use: http://spiedl.org/terms

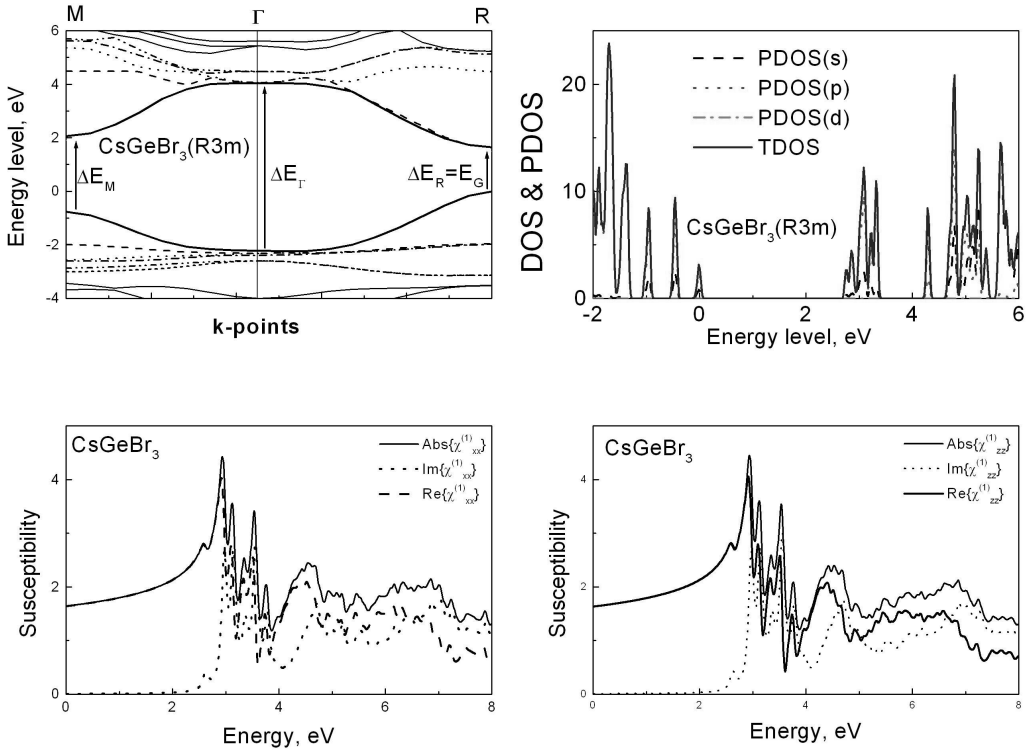

Figure 2. Results for the calculated electronic band structure, projected density of state (PDOS), frequency-dependent dielectric function on xx and zz components of rhombohedral $CsGeBr_3$. Partial densities of states (PDOS) of $CsGeBr_3$ projected onto all species at various atomic orbitals.

Table 2. Distorted structural factors were listed from the experimental and the First-Principles calculated lattice constants of the Rhombohedral NLO crystals $CsGeX_3$.

	$\Delta\alpha$	d_{Ge}	d_X
CGC (exp.)	3.077(7)	1.90	5.390(6)
CGB (exp.)	13.955(5)	2.36	2.721(9)
CGI (exp.)	15.555(5)	2.97	1.258(6)
CGC (calc.)	9.766(6)	2.01	5.866(7)
CGB (calc.)	18.922(2)	3.00	3.189(5)
CGI (calc.)	26.055(5)	3.54	1.407(7)

of the peaks in the calculated function is overestimated in part due to the exclusion of the effects of a finite relaxation time. Second, the experimental results in Table 3 were taken at room temperature; experimental work suggests that peak positions shift to higher energy at lower temperatures.[38]

Plot of second-order optical response in $CsGeBr_3$ of abslute second-order nonlinear optical susceptibility $\chi^{(2)}_{zzz}$ and $\chi^{(2)}_{zxx}$ was shown in figure 5. Major resonant period was found to be located around band-edge in both $\chi^{(2)}_{zzz}$ and $\chi^{(2)}_{zxx}$ tensors, respectively. Another group of significant peaks was happened at the half of the bandgap value, i.e. $\hbar\omega/2$ contribution. To go further, imaginary and real parts of second-order optical response in $CsGeBr_3$ of second-order nonlinear optical susceptibility $\chi^{(2)}_{zxx}$ and $\chi^{(2)}_{zzz}$ components. Both imaginary and real parts were

Downloaded From: http://proceedings.spiedigitallibrary.org/ on 01/21/2013 Terms of Use: http://spiedl.org/terms

also projected into four contribution, i.e. one- and two- photons of interband, and one- and two- photons of intraband in figures 3 and 4. The two-photon, 2ω, response was contributed out of phase with the one-photon, 1ω, response in the interband analysis in both $\chi^{(2)}_{zzz}$ and $\chi^{(2)}_{zxx}$ tensors and both imaginary and real parts. The half-photon, $\omega/2$, response was also significant in the interband and intraband analysis. They were due both structural and electronic properties, respectively. There were two significant peaks found in each second-order nolinear optical susceptibily. First group of significant peaks were observed around the CGX bandgap values. The other group of peaks were deviated from and were lower than zero-photon-energy (frequency) according to the degree of distortion, e.g. $d^{CGC}_{Ge,cal} : d^{CGB}_{Ge,cal} : d^{CGI}_{Ge,cal} \approx 4 : 6 : 7$. The magnitudes and energy levels of deviated peaks were found to be 31.72pm/V at -0.75eV for CGC, 00, -46.73pm/V at -1.15eV for CGB, and -93.86pm/V at -1.35eV for CGI, respectively. It is evident from Fig. **??** that our calculation predicts the peak positions lower in energy than those in the experimental results. All *ab initio* calculations share a difficulty in correctly predicting both the band gap and the peak positions in the linear response spectrum. The original first-principles work of Wang and Klein[39] employed the LDA and achieved some agreement in peak positions, but underestimated the fundamental band gap.

There are some reasons for the significant SHG signals of rhombohedral $CsGeX_3$ crystal. First of all, the SHG responses were contributed from the structural distortion and the off-centered Ge ion in the unit cell. The cell angle distortion of CGB is larger than that of CGC. The position of B-site cation, Ge, is closer to cell corner than that of CGC. The $\chi^{(2)}_{zzz}$ increases as these distortions increases. Secondly, the band-gap values decreased[6,33–37] and the NLO susceptibilities increased when the atomic weights of halides increased. The $\chi^{(2)}_{ijk}$ is approximately inverse-proportional to the cubic of band-gap value.[15,40,41] (see Eq. **??**) The third contribution has also been suggested that the electron lone-pair, the unbonding electron pair, of Ge which was polarized in [111] direction could give more contribution on the MME summation. The lone-pair polarization was also mentioned in G. Thiele *et al*'s reports.[33–37] These reasons could form the important guidelines for further NLO crystal designation.

According equation 6, the absolute values of the SHG susceptibility, $\chi^{(2)}_{ijk}(\beta, E)$, were plotted in Fig. 5 for $CsGeX_3$. Experimental data at energies above the gap are very scarce for the materials considered here. The only data were listed in Table 3. The calculated energy bandgap were about 30% smaller than the experimental observation; however, this is to be expected at the level of the LDA methodology. The smaller bandgap also overestimates optical dielectric constants. Although the smaller bandgap obtained with LDA can be corrected with a simple scissors approximation or more sophisticated GW correction, we did not intend to do so in this study. Our calculated second-order susceptibilities agreed reasonably well with available calculated and experimental results. Based on these comparisons, we can confidently conclude that the simulation results reported in this study reliably reflect the real physical properties of the ternary halides.

4. CONCLUSIONS

We have presented results for linear and second-order optical response in $CsGeX_3$ based on a first-principles FLAPW electronic structure calculation. We have employed a response formalism that is free of any unphysical divergences at zero frequency, providing believable results across the entire energy spectrum for any response function. Within this formalism we have implemented the scissors approximation, and have fully accounted for the modification of the velocity matrix elements that appear more explicitly in other calculation schemes. The response function expressions within the scissors approximation are straightforward to obtain, and are no less amenable to computation than without the scissors correction.

Our results for the imaginary part of the dielectric function $\epsilon_{ij}(\omega)$ show only reasonable agreement with experiment across a broad energy range, although we obtain excellent agreement with experiment for $\epsilon_{ij}(0)$. This illustrates the possible limitations of the scissors approximation and indicates that good zero-frequency results do not necessarily imply a good prediction of the dispersion of the dielectric function. The SHG susceptibility has

Downloaded From: http://proceedings.spiedigitallibrary.org/ on 01/21/2013 Terms of Use: http://spiedl.org/terms

been presented and it shows important differences from other theoretical calculations. The lack of experimental data, as well as its contradictory nature, prevents any conclusive comparison with experiment over a large energy range.

Ab initio calculations on $CsGeBr_3$ were also carried out to analyze the related electronic and optical properties. Space group symmetry of rhombohedral $CsGeBr_3$ was found to be $R3m$ (No. 160) and had no inversion center. The reflection powder second harmonic generation measurement of CGBr also showed that its nonlinear optical efficiency was larger than that of rhombohedral $CsGeCl_3$ by about 1.62 times and KDP by about 9.63 times. Saturated PSHG integration results of increasing powder particle sizes revealed that rhombohedral $CsGeBr_3$ was phase-matchable. The infrared transparent spectrum of rhombohedral $CsGeBr_3$ was extended to more than $22.5\mu m$. The rhombohedral $CsGeBr_3$ can be applied to infrared region as a potential nonlinear optical element.
Direct effects of structuraal distortion and electronic properties for linear and second-order optical response in $CsGeX_3$ based on a first-principles electronic structure calculation were presented . A response formalism that is free of any unphysical divergences were employed at zero frequency, providing believable results across the entire energy spectrum for any response function. Within this formalism, the response function expressions without the scissors approximation are straightforward to obtain. Our results for the imaginary part of the dielectric function show only reasonable agreement with experiment across a broad energy range, although we obtain excellent agreement with experiment for $\chi^{(2)}_{xyz}(\omega;\omega,0)$. This illustrates the possible limitations of the scissors approximation and indicates that good zero-frequency results do not necessarily imply a good prediction of the dispersion of the dielectric function. The SHG susceptibility has been presented and it shows important differences from other theoretical calculations. The lack of experimental data, as well as its contradictory nature, prevents any conclusive comparison with experiment over a large energy range.

This both gives us confidence in our calculated results, andXwhatever the status of our calculationX-encourages us to urge our experimental colleagues to reinvestigate the SHG susceptibility both at low frequency and over a wide frequency range. According to the powder X-ray diffraction pattern and powder SHG results, an innovative infrared nonlinear optical crystal $CsGeBr_3$, which was characterized as a rhombohedral crystal structure, was synthesized.

The structural deformed factors, $\Delta\alpha$, d_{Ge}, d_X were proposed to express the degree of the distortion from an ideal perovskite structure. $\Delta\alpha$ and d_{Ge} increased when the halide anions were changed from Cl (3.67eV) to I (1.53eV); in the mean while, the position deviated degree of the halide anion, d_X, decreased. The direct structural distortion effect on these rhombohedral CGXs were found in the First-Principles calculation results. The dielectric function and the second harmonic generation response coefficient behaved in the same manner as $\Delta\alpha$ and d_{Ge}. The direct bandgaps, E_G, of $CsGeX_3$ were all observed at R-point, ΔE_R. The bandgap values of CGX became smaller, i.e. $E_G^{CGC} > E_G^{CGB} > E_G^{CGI}$, as soon as the $\Delta\alpha$ and d_{Ge} increased, i.e. $d_{Ge}^{CGC} < d_{Ge}^{CGB} < d_{Ge}^{CGI}$. Partial density of states (PDOS) analysis were revealed that the valence band maximun (VBM) and conduction band minimum (CBM) were mainly contributed from the p-orbital of Germanium.

The magnitudes of $\chi^{(2)}_{ijk}$ were in the same manner with some reported experiment near the band gap. The First-Principle calculated magnitudes of both dielctric constant and second-harmonic generation were increased as well as the $\Delta\alpha$ and d_{Ge} increased. In summary, the lattice deviated angle and the position of Ge played the key roles on the linear and nonlinear optical responses.

ACKNOWLEDGMENTS

The authors are very grateful to Professor Henry Krakauer of the College of William and Mary for providing us with the FLAPW program, as well as for helpful discussions on making LDA calculations. We also acknowledge useful discussions with Dr. Clardio Aversa of the University of California at Santa Barbara. This work was

Downloaded From: http://proceedings.spiedigitallibrary.org/ on 01/21/2013 Terms of Use: http://spiedl.org/terms

Table 3. Calculated optical properties, the linear and second order optical responses, in $CsGeX_3$ at zero frequency. Non-linear optical coefficients of NLO crystals $CsGeX_3$ (X=Cl, Br, and I). They were compared with some available experimental data. The contribution of each specimen were projected to $\chi^{(2)}_{xzx}$, $\chi^{(2)}_{yyy}$, $\chi^{(2)}_{zxx}$, and $\chi^{(2)}_{zzz}$ in rhombohedral $CsGeX_3$.

NLO crystal	$CsGeCl_3$	$CsGeBr_3$	$CsGeI_3$	
$E_{g,exp}$	3.67	2.32	1.53	
$E_{g,cal}$	2.26(5)	1.49(1)	1.01(6)	direct, R-point
ϵ'	4.8598(5)	5.2521(1)	6.5313(4)	unpolarized, zero-frequency
ϵ'	4.8623(7)	5.2526(6)	6.5330(9)	unpolarized, Sum-rule
ϵ'_{zz}	8.8477(5)	10.183(0)	12.551(4)	zero-frequency
ϵ'_{xx}	6.6550(5)	7.5836(7)	9.5420(6)	zero-frequency
$d^{(2)}_{eff,exp}$	2.12	3.46	NA	(pm/V)
$\chi^{(2)}_{zzz}$	11.64924	22.39020	127.7794	zero-frequency (pm/V)
$\chi^{(2)}_{yyy}$	7.706676	7.041843	33.39160	zero-frequency (pm/V)
$\chi^{(2)}_{zxx}$	2.629566	2.672494	4.590949	zero-frequency (pm/V)
$\chi^{(2)}_{xzx}$	2.629567	2.672494	4.590949	zero-frequency (pm/V)

supported by the Natural Sciences and Engineering Research Council of Canada and the Ontario Laser and Lightwave Research Centre. The authors are indebted to the financial support from the National Science Council of the Republic of China under both grants, NSC 94-2112-M-009-033 and NSC 94-2212-E-014-004. Address any correspondence to C. S. Chang. (cschang@mail.nctu.edu.tw) or L. C. Tang. (newton4538.eo85g@nctu.edu.tw). This unnumbered section is used to identify those who have aided the authors in understanding or accomplishing the work presented and to acknowledge sources of funding.

References

REFERENCES

1. D. M. Burland *Chem. Rev.* **94**, p. 1, 1994.
2. J. Z. *in* D S Chemla and J Zyss, *Nonlinear Optical Properties of Organic Molecules and Crystals*, Academic Press, Orlando, 1987.
3. J. Zhang. PhD thesis, Wuhan University, Department of Material Science, 1995.
4. M. D. Ewbank, F. Cunningham, R. Borwick, M. J. Rosker, and P. Gunter *CLEO97 paper* **CFA7**, p. 462, 1997.
5. J. Zhang, N. Su, C. Yang, J. Qin, N. Ye, B. Wu, and C. Chen *Chem. Proc. SPIE* **3556**, p. 1, 1998.
6. L.-C. Tang, C.-S. Chang, and J. Y. Huang *J. Phys.: Condens. Matter* **12**, p. 9129, 2000.
7. Q. Gu, Q. Pan, W. Shi, X. Sun, and C. Fang *Progress in Crystal Growth and Characterization of Material* **40**, pp. 89–95, 2000.
8. Q. Gu, Q. Pan, X. Wu, W. Shi, and C. Fang *Journal of Crystal Growth* **212**, pp. 605–607, 2000.
9. Q. Gu, C. Fang, W. Shi, X. Wu, and Q. Pan *Journal of Crystal Growth* **225**, pp. 501–504, 2001.
10. L. C. Tang, J. Y. Huang, C. S. Chang, M. H. Lee, and L. Q. Liu *J. Phys.: Condens. Matter* **17**, p. 7275, 2005.
11. P. Ren, J. Qin, and C. Chen *Inorganic Chemistry* **42**, pp. 8–10, 2003.
12. V. M. Goldschmidt *Ber. Dtsch. Chem. Ges.* **60**, p. 1263, 1927.
13. V. M. Goldschmidt *Fortschr. Min.* **15**, p. 73, 1931.
14. V. G. Dmitriev, G. G. Gurzadyan, and D. N. Nikogosyan, *Handbook of Nonlinear Optical Crystals, third ed.*, Springer-Verlag, Berlin, 1999.

Downloaded From: http://proceedings.spiedigitallibrary.org/ on 01/21/2013 Terms of Use: http://spiedl.org/terms

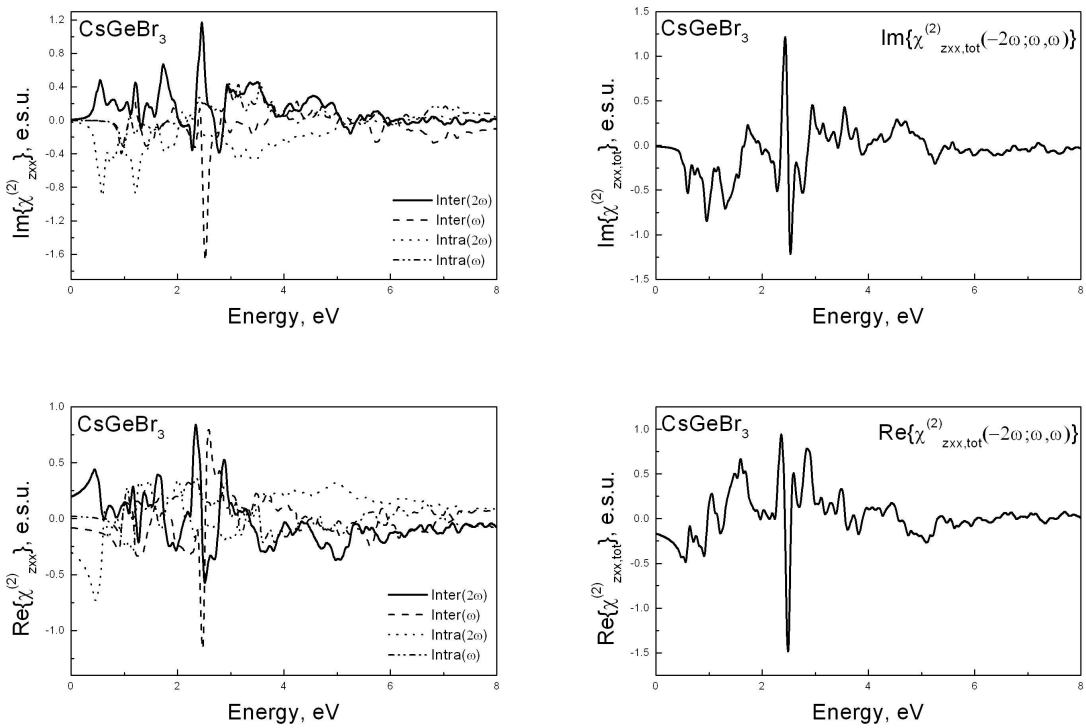

Figure 3. Imaginary and real parts of second-order optical response in $CsGeBr_3$ of second-order nonlinear optical susceptibility $\chi^{(2)}_{zxx}$. Both imaginary and real parts were also projected into four contribution, i.e. one- and two- photons of interband, and one- and two- photons of intraband,

15. R. W. Boyd, *Nonlinear Optics 2nd ed.*, Academic Press, Boston,MA, 2003.
16. J. F. Nye, *Physical Properties of Crystals*, Oxford University Press, Oxford, 1957.
17. J. E. Sipe and E. Ghahramani *Phys. Rev. B* **48**, p. 11705, 1993.
18. C. Aversa and J. E. Sipe *Phys. Rev. B* **52**, p. 14636, 1995.
19. A. D. Corso and F. Mauri *Phys. Rev. B* **50**, p. 5756, 1994.
20. D. J. Moss, J. E. Sipe, and H. M. van Driel *Phys. Rev. B* **36**, p. 1153, 1987.
21. D. J. Moss, E. Ghahramani, J. E. Sipe, and H. M. van Driel *Phys. Rev. B* **41**, p. 1542, 1990.
22. E. Ghahramani, D. J. Moss, and J. E. Sipe *Phys. Rev. B* **43**, p. 8990, 1991.
23. E. Ghahramani, D. J. Moss, and J. E. Sipe *Phys. Rev. B* **43**, p. 9700, 1991.
24. D. J. Moss, E. Ghahramani, and J. E. Sipe *Phys. Status Solidi B* **164**, p. 587, 1991.
25. Z. H. Levine and D. C. Allan *Phys. Rev. B* **44**, p. 12781, 1991.
26. F. S. Galasso, *Perovskites and High t Superconductors*, Gordon and Breach Scientific Publications, New York, 1990.
27. V. Butler, C. R. Catlow, B. E. F. Fender, and J. H. Harding *Solid State Ionics* **8**, p. 109V113, 1982.
28. L. G. Tejuca, J. L. G. Fierro, and J. M. D. Tascon *Adv. Catal.* **36**, p. 237V328, 1989.
29. H. Yokokawa, N. Sakai, T. Kawada, and M. Dokiya *Solid State Ionics* **52**, p. 43V56, 1992.
30. N. W. Thomas *Br. Ceram. Trans.* **96**, p. 7V15, 1997.
31. R. D. Shannon and C. T. Prewitt *Acta Cryst.* **B25**, p. 925, 1969.
32. R. D. Shannon *Acta Cryst.* **A32**, p. 751V767, 1976.
33. U. Schwarz, H. Hillebrecht, M. Kaupp, K. Syassen, H.-G. von Schnering, and G. Thiele *Journal of Solid State Chemistry* **118**, pp. 20–27, 1995.
34. U. Schwarz, F. Wagner, K. Syassen, and H. Hillebrecht *Phys. Rev. B* **53**(19), p. 12545, 1996.

Downloaded From: http://proceedings.spiedigitallibrary.org/ on 01/21/2013 Terms of Use: http://spiedl.org/terms

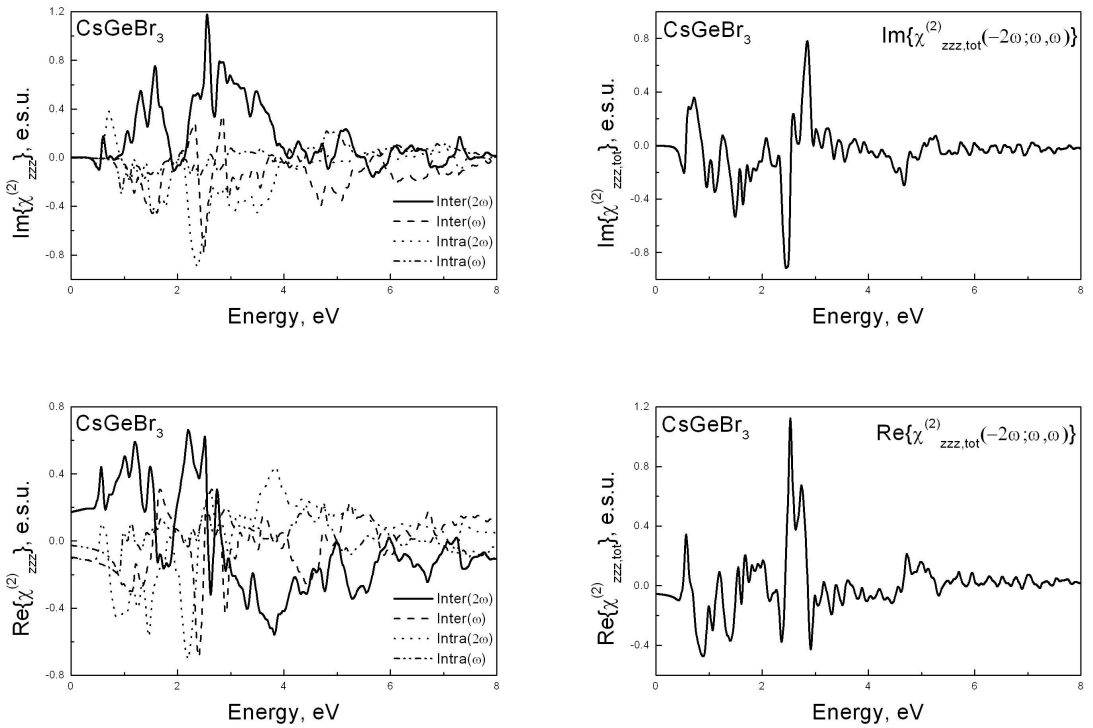

Figure 4. Imaginary and real parts of second-order optical response in $CsGeBr_3$ of second-order nonlinear optical susceptibility $\chi^{(2)}_{zzz}$. Both imaginary and real parts were also projected into four contribution, i.e. one- and two- photons of interband, and one- and two- photons of intraband,

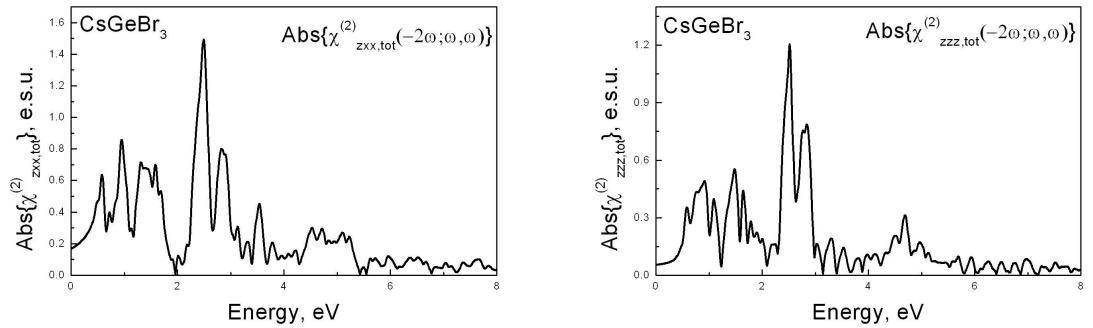

Figure 5. Plot of second-order optical response in $CsGeBr_3$ of abslute second-order nonlinear optical susceptibility $\chi^{(2)}_{zzz}$ and $\chi^{(2)}_{zxx}$.

35. G. Thiele, H. W. Rotter, and K. D. Schmidt *Z. Anorg. Allg. Chem.* **545**, p. 148, 1987.
36. G. Thiele, H. W. Rotter, and K. D. Schmidt *Z. Anorg. Allg. Chem.* **559**, pp. 7–16, 1988.
37. D.-K. Seo, N. Gupta, M.-H. Whangbo, H. Hillebrecht, and G. Thiele *Inorg. Chem.* **37**, p. 407, 1998.
38. P. Lautenschlager, M. Garriga, S. Logothetidis, and M. Cardona *Phys. Rev. B* **35**, p. 9174, 1987.
39. C. S. Wang and B. M. Klein *Phys. Rev. B* **24**, p. 3417, 1981.
40. B. Champagne and D. M. Bishop *Advances in Chemical Physics* **126**, p. 41, 2003.
41. Y. R. Shen, *The Principles of Nonlinear Optics*, John Wiley and Sons, 2002.

Downloaded From: http://proceedings.spiedigitallibrary.org/ on 01/21/2013 Terms of Use: http://spiedl.org/terms